Theor Chim Acta (1995) 91: 267–289

Theoretica Chimica Acta

Analytic energy derivatives for the equation-of-motion coupled-cluster method: Algebraic expressions, implementation and application to the S_1 state of HFCO

John F. Stanton[1], Jürgen Gauss[2]

[1] Institute for Theoretical Chemistry, Departments of Chemistry and Biochemistry, The University of Texas at Austin, Austin, TX 78712, USA

[2] Lehrstuhl für Theoretische Chemie, Institut für Physikalische Chemie, Universität Karlsruhe, D-76128 Karlsruhe, Germany

Received July 6, 1994/Accepted October 13, 1994

Summary. The general theory of analytic derivatives for the equation-of-motion coupled cluster (EOM-CC) method is reviewed. Special attention is paid to the EOM-CC singles and doubles (EOM-CCSD) approximation, which has the same computational scaling properties as the coupled-cluster singles doubles (CCSD) ground state method and is therefore applicable to a wide range of molecular systems. The detailed spin orbital equations that must be solved in EOM-CCSD gradient calculations are presented for the first time, and some guidelines are discussed regarding their computational implementation. Finally, use of the EOM-CCSD gradient method is illustrated by determining the structure, dipole moment components, harmonic frequencies and infrared intensities of formyl fluoride (HFCO) in its singlet excited (n, π^*) state.

Key words: Analytic energy derivatives—Equation-of-motion coupled-cluster method

1 Introduction

The reliable characterization of potential energy surfaces for excited electronic states is one of the most important and challenging frontiers for modern quantum chemistry. Due to the participation of these systems in essentially all laser spectroscopic experiments and prospects of controlling chemical reactions by selective involvement of intermediate electronic levels, there is an increasing need for detailed understanding of molecular excited states and their properties. For various reasons, information provided by theory in this area has not kept pace with that for processes that occur strictly on the lowest adiabatic surface of a given symmetry and spin multiplicity, where standard easy-to-use methods for highly accurate calculations are widely available.

Traditionally, the most successful quantum chemical treatments of excited states have been based on multiconfigurational zeroth-order wave functions [1], often augmented by additional configuration interaction (CI) [2–6] or perturbation theory [7, 8] to account for dynamical electron correlation effects. In principle, correlated multireference calculations are able to describe electronic wave functions accurately for both ground and excited states over a wide range of molecular

geometries. However, the ease of applying these methods to chemical problems is mitigated by several factors. For one, the cost required to maintain a consistent level of accuracy scales approximately factorially with the number of valence electrons in the system; accurate calculations for molecules with more than a few nonhydrogen atoms can therefore be very expensive. Another consideration is that construction of a suitable zeroth-order wave function may be difficult, since slight adjustments in the active space can profoundly affect the results. Although some successful strategies have been developed for dealing with difficult situations [9], accurate calculations of excited state properties are not easy to perform with correlated multireference methods and are mostly left to specialists.

One technique free of some of the problems discussed above is the equation-of-motion coupled-cluster (EOM-CC) method, originally outlined by Monkhorst [10] and subsequently developed by several others [11–22]. Difficulties associated with the selection of an appropriate zeroth-order wave function are circumvented in these calculations by basing the parameterization on a ground state [23] that does not mix with the level(s) of interest [24]. In the most practical realization of EOM-CC, the coupled-cluster singles and doubles (CCSD) method [25] is used to obtain a correlated wave function for the ground state. The wave function parameters are then used as the basis for a similarity transformation of the electronic Hamiltonian. The resulting transformed Hamiltonian ($\bar{H}$) is finally diagonalized in the subspace of quasiparticle states comprised of the Slater determinant reference for the ground state and those related to it by promotion of one or two electrons. Energy levels and the electronic structure of excited states determined by the diagonal representation of $\bar{H}$ are demonstrably superior to those obtained from the bare electronic Hamiltonian (standard single reference CI) in the same determinantal basis [16, 18–21]. Moreover, unphysical scaling of the energy with respect to the number of electrons in the system – a characteristic failure of all truncated CI approaches – is avoided in EOM-CC due to the block upper triangular structure of the transformed Hamiltonian [26]. The EOM-CCSD model is more easily applied to chemical problems than multireference techniques since the task of constructing a zeroth-order wave function in the latter is replaced by a simpler and often less costly evaluation of the ground state CCSD wave function. Nevertheless, the desirable balanced nature of multireference methods is retained to some extent in EOM-CC, especially in cases where the singly and doubly excited quasiparticle configurations that constitute the basis of $\bar{H}$ represent adequate approximations to the final states of interest.

The accuracy of EOM-CCSD is competitive with large-scale correlated multireference calculations when two criteria are met. First, non-dynamical electron correlation effects in the ground state must be small enough that the CCSD wave function does not differ significantly from the exact result. In addition, the excited states of interest should be adequately characterized as single excitations relative to the ground state. A practical limitation imposed by these requirements is that the EOM-CCSD model is not generally capable of consistent accuracy over a complete potential energy surface, especially asymptotic regions associated with homolytic bond breaking. The reason for this is that the single determinant starting point for the ground state CCSD calculation is not even qualitatively correct in these situations and the accuracy of the ground state wave function may be severely compromised [27]. However, when applied to the study of excited state structures in the Franck–Condon region or to the characterization of isomers on the excited state potential energy surface, the EOM-CCSD method can be expected to give accurate results when the criteria above are met, as illustrated by existing

applications [28–31]. Finally, when the ground state is adequately represented by the single determinant CCSD method, it should be noted that the "singly excited" states described most accurately by EOM-CCSD are precisely those that most chemists are interested in – low-lying levels accessible from the ground state by one photon processes.

It is widely appreciated that an efficient scheme for evaluating analytic energy derivatives is a prerequisite for any method that is intended for the routine study of molecular potential energy surfaces [32]. While the potential function and position of local minima and transition states can be determined by performing energy calculations over a grid of points, such a procedure is inefficient and finally becomes intractable for molecules that contain more than a few atoms. However, exploration of the surface is greatly facilitated if the energy gradient can be calculated for a cost that does not scale appreciably with the number of geometrical degrees of freedom. An interest in potential energy surfaces for molecules in excited electronic states was the impetus for recent work which culminated in the formulation of an analytic gradient strategy for EOM-CC calculations and its implementation at the EOM-CCSD level of theory [33, 34]. Hence, this powerful method can now be applied to investigations of excited states in much the same way that standard correlated methods (essentially all of which have accompanying analytic gradient extensions) are used to treat ground state chemistry.

The formalism for EOM-CC gradients presented in Ref. [33] applies to methods defined by any truncation of the ground state CC wave function and diagonalization space. However, the equations presented in that work are based on general operators and do not provide a basis for implementation of energy derivatives for specific truncated approximations. For methods such as EOM-CCSD, working equations are obtained by expanding the abstract operator expressions in terms of fundamental quantities expressed in the representation of molecular spin orbitals. The principal objectives of this paper are to document the explicit equations that must be solved to calculate EOM-CCSD energy derivatives analytically and to discuss some practical guidelines that simplify their implementation. In addition, use of the method is illustrated by determining the structure and properties of formyl fluoride (HFCO) in its singlet (n, π^*) excited state.

2 Theory

It is appropriate to begin our discussion of EOM-CCSD gradient theory by summarizing some of the notation that will be used in this section. Following a common convention, spin orbitals occupied in the zeroth-order Slater determinant that approximates the ground state wave function ($|0\rangle$) are designated by the labels $i, j, k, \ldots$, while $a, b, c \ldots$ specify unoccupied levels. In some equations, it will be convenient to refer to orbitals that may be either occupied or unoccupied in the reference determinant; the generic indices $p, q, r \ldots$ are reserved for this purpose. The complete space of Slater determinants comprising $|0\rangle$ and those obtained from it by all possible promotion of electron(s) from occupied to unoccupied orbitals is specified by $\boldsymbol{h}$. Specific subspaces of $\boldsymbol{h}$ that will be invoked in the following are defined by

$\boldsymbol{g}$: All determinants obtained from $|0\rangle$ by promotion of one or two electrons.

$\boldsymbol{q}$: All determinants obtained from $|0\rangle$ by promotion of more than two electrons.

$\boldsymbol{p}$: The diagonalization space $[|0\rangle \oplus \boldsymbol{g}]$.

Ground state coupled-cluster theory [25, 35–37] and its extension to calculate derivatives of the energy analytically [38–49] are discussed at length in the literature and the reader is assumed to be familiar with these subjects. Similarly, details pertaining to the EOM-CCSD parameterization of excited state wave functions and the construction of the similarity transformed Hamiltonian will not be presented since these topics are also treated adequately elsewhere [19]. Rather, we specialize to analytic derivatives of the EOM-CCSD energy and focus on aspects of these calculations that require theoretical insight or analysis of operator expressions that are not encountered in ground state CC theory. Therefore, mastery of the subject matter of this paper coupled with a knowledge of standard CCSD gradient approaches should allow experienced computational quantum chemists to implement our EOM-CCSD gradient formalism rather easily.

In EOM-CCSD theory, electronic states are obtained by diagonalizing the (non-Hermitian) similarity transformed Hamiltonian $\bar{H}$ defined by

$$\bar{H} \equiv \exp(-T) H \exp(T). \tag{1}$$

In Eq. (1), H is the bare electronic Hamiltonian and T is the cluster operator that defines the ground state wave function via the usual CC ansatz

$$|\Psi_{\text{ref}}\rangle = \exp(T)|0\rangle, \tag{2}$$

which implies

$$E_{\text{ref}} = \langle 0|\bar{H}|0\rangle. \tag{3}$$

Electronic energies can be written as biorthogonal expectation values

$$E = \langle \tilde{\Psi}|H|\Psi\rangle \tag{4}$$

$$= \langle 0|\mathscr{L}\exp(-T)H\exp(T)\mathscr{R}|0\rangle \tag{5}$$

$$= \langle 0|\mathscr{L}\bar{H}\mathscr{R}|0\rangle, \tag{6}$$

where $\mathscr{L}$ and $\mathscr{R}$ are left- and right-hand eigenvectors of $\bar{H}$

$$\mathscr{L} = \mathscr{L}_0 + \mathscr{L}_1 + \mathscr{L}_2 \tag{7}$$

$$= l_0 + \sum_{ai} l_a^i i^\dagger a + \frac{1}{4}\sum_{abij} l_{ab}^{ij} i^\dagger a j^\dagger b; \tag{8}$$

$$\tag{9}$$

$$\mathscr{R} = \mathscr{R}_0 + \mathscr{R}_1 + \mathscr{R}_2 \tag{10}$$

$$= r_0 + \sum_{ai} r_i^a a^\dagger i + \frac{1}{4}\sum_{abij} \gamma_{ij}^{ab} a^\dagger i b^\dagger j. \tag{11}$$

that parameterize (together with $\exp(-T)$ and $\exp(T)$, respectively [19]) the final bra and ket state wave functions. For the purpose of clarifying subsequent discussion, we point out that the correlated CCSD ground state is contained in the spectrum of $\bar{H}$, namely the root for which $\mathscr{R} = r_0 = 1$ [all $r_i^a = r_{ij}^{ab} = 0$] and where $\mathscr{L}$ is the Λ vector introduced by Arponen [50] and later exploited by Adamowicz

et al. [38] to simplify the calculation of CC energy derivatives. Hence, any set of equations for EOM-CCSD gradients must reduce to those of CCSD theory when the $\mathscr{R}$ and $\mathscr{L}$ amplitudes assume these values. Note that biorthogonality of the excited and ground states in EOM-CC [12] mandates that $l_0 = 0$ for the former, while r_0 need not vanish.

Straightforward differentiation of the energy functional (Eq. (6)) with respect to the perturbation χ yields

$$\frac{\partial E}{\partial \chi} = \langle 0| \frac{\partial \mathscr{L}}{\partial \chi} \bar{H} \mathscr{R}|0\rangle + \langle 0| \mathscr{L} \bar{H} \frac{\partial \mathscr{R}}{\partial \chi}|0\rangle + \langle 0| \mathscr{L} \bar{H} \frac{\partial T}{\partial \chi} \mathscr{R}|0\rangle - \langle 0| \mathscr{L} \frac{\partial T}{\partial \chi} \bar{H} \mathscr{R}|0\rangle + \langle 0| \mathscr{L} \exp(-T) \frac{\partial H}{\partial \chi} \exp(T) \mathscr{R}|0\rangle. \tag{12}$$

While this expression could serve as the basis for a computational implementation of EOM-CCSD energy derivatives, the formalism would be of no practical use since all but the last term necessitate iterative steps that scale with the sixth power of the basis set dimension (the same scaling properties as the CCSD method) and furthermore require separate solutions for each degree of freedom. It is easy to show that the sum of the first two terms vanishes due to biorthonormality of the final states, but those that include $\partial T/\partial \chi$ remain since the energy is not stationary with respect to first-order changes in the cluster amplitudes. However, it has been shown [33] that the Dalgarno–Stewart double interchange technique [51] can be used to eliminate these terms in favor of an additional perturbation independent linear operator $\mathscr{L}$. Matrix elements (amplitudes) of this deexcitation operator

$$\mathscr{L} \equiv \mathscr{L}_1 + \mathscr{L}_2 \tag{13}$$

$$= \sum_{ai} \zeta_a^i i^\dagger a + \frac{1}{4} \sum_{abij} \zeta_{ab}^{ij} i^\dagger a j^\dagger b \tag{14}$$

are determined by solving the system of linear equations

$$\langle 0| \mathscr{L} |\boldsymbol{p}\rangle = -\langle 0| \Xi |\boldsymbol{p}\rangle [\langle \boldsymbol{p}| \bar{H} - E_{\text{ref}} |\boldsymbol{p}\rangle]^{-1}, \tag{15}$$

where matrix elements of Ξ

$$\Xi \equiv \Xi_1 + \Xi_2 \tag{16}$$

$$= \sum_{ai} \xi_a^i i^\dagger a + \frac{1}{4} \sum_{abij} \xi_{ab}^{ij} i^\dagger a j^\dagger b \tag{17}$$

are numerically equal to the first derivative of the energy with respect to the T cluster amplitudes. It is rather easily demonstrated that this operator is completely determined by contractions amongst $\mathscr{L}$, $\mathscr{R}$ and $\bar{H}$ involving intermediate states that lie outside the space spanned by $\boldsymbol{p}$ [33],

$$\langle 0| \Xi |\boldsymbol{p}\rangle = \langle 0| \mathscr{L} \bar{H} |\boldsymbol{q}\rangle \langle \boldsymbol{q}| \mathscr{R} |\boldsymbol{p}\rangle. \tag{18}$$

Note that Eq. (18) implies that the ξ amplitudes vanish both for the ground state (where $\mathscr{R} = r_0 = 1$ and therefore cannot connect determinants belonging to the

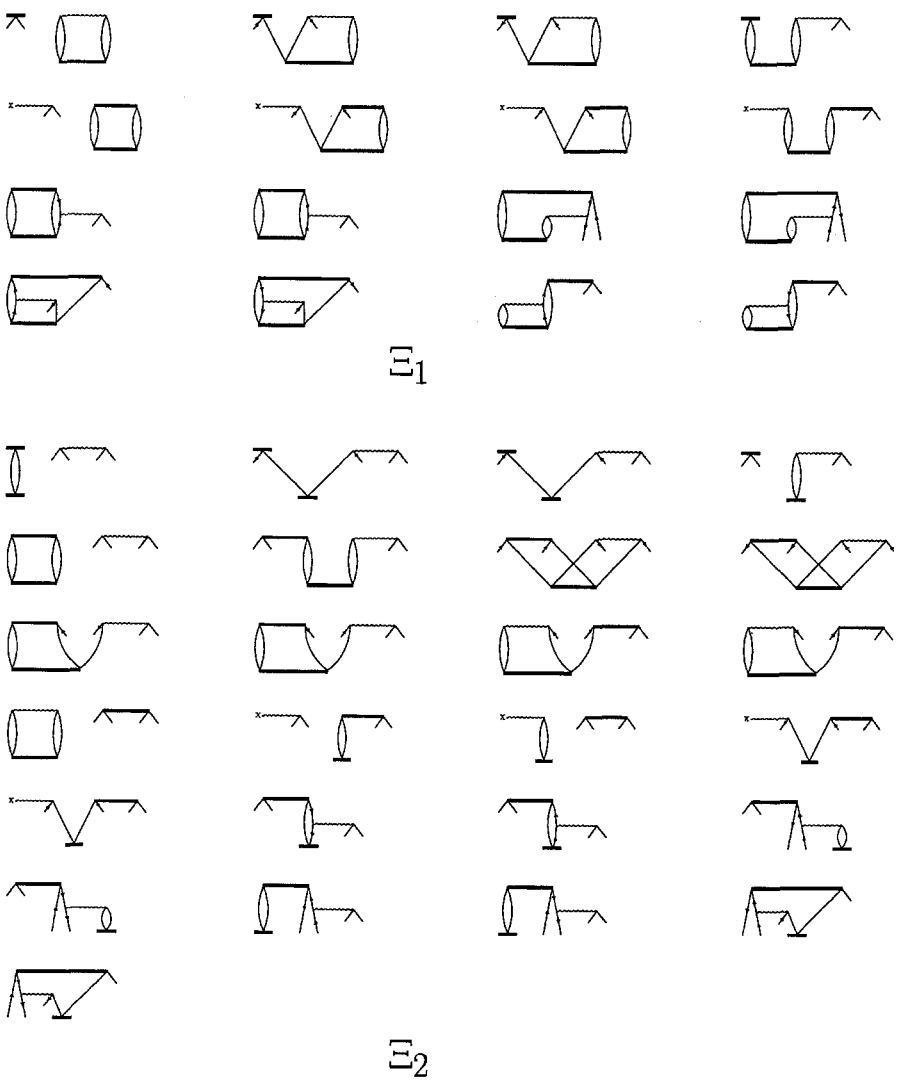

Fig. 1. Diagrammatic representation of the Ξ amplitude equations, which are also documented algebraically in Eqs. (19) and (20). The upper and lower thick lines correspond to the $\mathscr{L}$ and $\mathscr{R}$ operators, respectively, while the T cluster operator is represented by thin line. Matrix elements of the similarity transformed Hamiltonian $\bar{H}$ are designated by wavy interaction lines. Note that all diagrams involve triply and quadruply excited intermediate states

$\boldsymbol{p}$ and $\boldsymbol{q}$ subspaces) and in cases where the EOM-CCSD method is exact, namely for systems containing fewer than three electrons or with at most two unoccupied spin orbitals (where $\boldsymbol{q}$ is the null set). Terms contributing to Ξ are most easily enumerated with diagrammatic techniques since their use greatly simplifies analysis of the intermediate states. A complete set of diagrams for the Ξ_1 and Ξ_2 deexcitation amplitudes is given in Fig. 1. So that the treatment is applicable to both closed shell restricted and open shell reference determinants, antisymmetrized (or Brandow)

diagrams are used. Rules for translating the diagrams into corresponding spin orbital equations are given, for example, in Ref. [52]. The equivalent algebraic expressions are

$$\begin{aligned}\xi_a^i = &\tfrac{1}{4} l_a^i r_{mn}^{ef} W_{mnef} - \tfrac{1}{2} l_a^m r_{mn}^{ef} W_{inef} - \tfrac{1}{2} l_e^i r_{mn}^{ef} W_{mnaf} + l_e^m r_{mn}^{ef} W_{inaf} \\ &+ \tfrac{1}{4} l_{ef}^{mn} r_{mn}^{ef} F_{ia} - \tfrac{1}{2} l_{ef}^{in} r_{mn}^{ef} F_{ma} - \tfrac{1}{2} l_{af}^{mn} r_{mn}^{ef} F_{ie} + l_{af}^{in} r_{mn}^{ef} F_{me} \\ &- \tfrac{1}{2} l_{ef}^{mn} r_{mo}^{ef} W_{oina} + \tfrac{1}{2} l_{ef}^{mn} r_{mn}^{eg} W_{figa} - l_{ea}^{mo} r_{mn}^{ef} W_{nifo} + l_{ge}^{im} r_{mn}^{ef} W_{gnaf} \\ &- \tfrac{1}{2} l_{ea}^{mn} r_{mn}^{fg} W_{eifg} - \tfrac{1}{2} l_{ef}^{io} r_{mn}^{ef} W_{mnoa} + \tfrac{1}{2} l_{ag}^{in} r_{mn}^{ef} W_{gmfe} - \tfrac{1}{2} l_{af}^{io} r_{mn}^{ef} W_{mneo} \end{aligned} \tag{19}$$

and

$$\begin{aligned}\xi_{ab}^{ij} = &l_e^m r_m^e W_{ijab} - P_-(ab) l_a^m r_m^e W_{ijeb} - P_-(ij) l_e^i r_m^e W_{mjab} + P_-(ij) P_-(ab) l_a^i r_m^e W_{mjeb} \\ &+ \tfrac{1}{4} l_{ef}^{mn} r_{mn}^{ef} W_{ijab} + P_-(ij) P_-(ab) l_{ae}^{im} r_{mn}^{ef} W_{jnbf} + \tfrac{1}{4} l_{ab}^{mn} r_{mn}^{ef} W_{ijef} + \tfrac{1}{4} l_{ef}^{ij} r_{mn}^{ef} W_{mnab} \\ &- \tfrac{1}{2} P_-(ab) l_{ea}^{mn} r_{mn}^{ef} W_{ijfb} - \tfrac{1}{2} P_-(ij) l_{ef}^{in} r_{mn}^{ef} W_{mjab} \\ &- \tfrac{1}{2} P_-(ab) l_{fb}^{ij} r_{mn}^{ef} W_{mnea} - \tfrac{1}{2} P_-(ij) l_{ab}^{mj} r_{mn}^{ef} W_{inef} \\ &+ \tfrac{1}{4} l_{ab}^{ij} r_{mn}^{ef} W_{mnef} + P_-(ij) P_-(ab) l_{eb}^{mj} r_m^e F_{ia} + l_{ab}^{ij} r_m^e F_{me} - P_-(ij) l_{ab}^{mj} r_m^e F_{ie} \\ &- P_-(ab) l_{eb}^{ij} r_m^e F_{ma} - P_-(ij) P_-(ab) l_{ae}^{in} r_m^e W_{mjnb} + P_-(ij) P_-(ab) l_{af}^{im} r_m^e W_{fjeb} \\ &+ P_-(ab) l_{af}^{ij} r_m^e W_{fmbe} - P_-(ij) l_{ab}^{in} r_m^e W_{jmne} + P_-(ij) l_{fe}^{im} r_m^e W_{fjab} \\ &- P_-(ab) l_{ea}^{mn} r_m^e W_{ijnb} - l_{ef}^{ij} r_m^e W_{fmba} - l_{ab}^{mn} r_m^e W_{ijen}, \end{aligned} \tag{20}$$

where the Einstein summation convention has been followed. In Eqs. (19) and (20), one- and two-body matrix elements of $\bar{H}$ [53] are designated by F and W, respectively. These quantities are defined in terms of T amplitudes, Fock matrix elements and antisymmetrized two-electron integrals and are documented in Table 1 of Ref. [19]. The antisymmetric permutation operator $P_-(rs)$ is defined by

Table 1. Time required (in seconds) for discrete stages of EOM-CCSD energy and energy + analytic gradient calculations for the $\tilde{A}$ state of vinylidene, using a triple-zeta plus double polarization basis set consisting of 78 contracted Gaussian functions. The calculation was performed in C_{2v} symmetry on an IBM RS-6000/370

	Energy calculation	Gradient calculation
Integral evaluation	35	35
SCF calculation	5	5
Integral transformation	31	31
Integral processing	9	9
Ground state CC equations	126	126
Evaluation of $\bar{H}$ elements	16	16
$\bar{H}$ diagonalization ($\mathscr{R}$)	62	62
Solution for $\mathscr{L}$	—	54
$\mathscr{L}$ equations	—	61
Density matrix evaluation	—	9
Transformation of Γ	—	8
Integral derivatives	—	102
Total	281	518

its action on a function of the arguments

$$P_-(rs)\mathscr{S}(pqrstu) \equiv \mathscr{S}(pqrstu) - \mathscr{S}(pqsrtu). \tag{21}$$

To facilitate comparison of the algebraic expressions with the diagrammatic representation of the Ξ amplitudes, terms in Eqs. (19) and (20) have been ordered so that a one-to-one correspondence exists between them and the diagrams in Fig. 1.

Once the ζ amplitudes are available, derivatives of the energy can be calculated from the equation [33]

$$\frac{\partial E}{\partial \chi} = \langle 0 | \mathscr{L} \exp(-T) \frac{\partial H}{\partial \chi} \exp(T) \mathscr{R} | 0 \rangle + \langle 0 | \mathscr{Y} \exp(-T) \frac{\partial H}{\partial \chi} \exp(T) | 0 \rangle. \tag{22}$$

Note that the second term does not contribute for the root corresponding to the CCSD ground state since both Ξ and $\mathscr{Y}$ vanish in this case. Meanwhile, the first term reduces to the gradient expression derived by Adamowicz et al. [38] for the CCSD method [with $\mathscr{L} = \Lambda$ and $\mathscr{R} = r_0 = 1$] as anticipated above. In passing, we point out that $\mathscr{Y}$ plays a somewhat different role than the Λ operator of CC gradient theory despite some superficial similarities. In the latter case, the λ amplitudes participate in the parameterization of a dual state that allows the energy and arbitrary first-order properties to be written as biorthogonal expectation values. This means that the gradient and properties such as the dipole moment can be calculated by contracting appropriate operators with the reduced density matrix defined by expectation values of creation and annihilation operators over the CC ket state (Eq. (2)) and its dual wave function, $\langle 0 | \Lambda \exp(-T)$ [54]. In EOM-CC theory, however, the $\mathscr{Y}$ operator does not lead to satisfaction of an analogous generalized Hellman–Feynman condition. Stated alternatively, the final state energies are not simultaneously stationary with respect to variation of the $\mathscr{L}$, $\mathscr{R}$ and T amplitudes. This is a consequence of the fact that the T amplitudes are determined for the ground state. In any event, the operator expression for the EOM-CC gradient (Eq. (22)) involves the first-order response of just the bare molecular orbital basis Hamiltonian. One can consequently evaluate the gradient by contracting an "effective" density D with matrix elements of the differentiated Fock operator and antisymmetrized two-electron integrals,

$$\frac{\partial E}{\partial \chi} = \sum_{pq} D_q^p \frac{\partial f_{qp}}{\partial \chi} + \sum_{pqrs} D_{rs}^{pq} \frac{\partial}{\partial \chi} \langle rs \| pq \rangle. \tag{23}$$

It is important to understand that an identical expression holds for analytic derivatives of the CCSD energy, in which D is simply the n-particle reduced density. In EOM-CC, however, D is not a true density (in the sense that it can be written as a biorthogonal expectation value [55]). Despite this distinction, the correspondence between gradient expressions for EOM-CCSD and CCSD suggests that similar computational strategies can be used for both methods. Indeed, once D has been evaluated, an existing CCSD gradient program can perform *all* subsequent steps needed to calculate EOM-CCSD energy derivatives! The remainder of this section therefore concentrates on evaluation of the one- and two-particle effective density matrix.

The sum of two distinct quantities constitutes the effective density of EOM-CC gradient theory – the actual reduced density consistent with the wave function parameterization (ρ) and a correction term ($\tilde{\rho}$) that accounts for the first-order

response of the ground state T amplitudes. From Eq. (22), one can infer that the one- and two-particle matrix elements of ρ and $\tilde{\rho}$ are defined by

$$\rho_q^p = \langle 0 | \mathscr{L} \exp(-T) p^\dagger q \exp(T) \mathscr{R} | 0 \rangle, \tag{24}$$

$$\rho_{rs}^{pq} = \langle 0 | \mathscr{L} \exp(-T) p^\dagger q^\dagger sr \exp(T) \mathscr{R} | 0 \rangle, \tag{25}$$

and

$$\tilde{\rho}_q^p = \langle 0 | \mathscr{L} \exp(-T) p^\dagger q \exp(T) | 0 \rangle, \tag{26}$$

$$\tilde{\rho}_{rs}^{pq} = \langle 0 | \mathscr{L} \exp(-T) p^\dagger q^\dagger sr \exp(T) | 0 \rangle, \tag{27}$$

respectively. Equations (26) and (27) are identical in form to those for the CCSD ground state density matrix

$$[D_q^p]_{\text{ref}} \equiv \langle 0 | \Lambda \exp(-T) p^\dagger q \exp(T) | 0 \rangle, \tag{28}$$

$$[D_{rs}^{pq}]_{\text{ref}} \equiv \langle 0 | \Lambda \exp(-T) p^\dagger q^\dagger sr \exp(T) | 0 \rangle, \tag{29}$$

except that Λ rather than $\mathscr{L}$ is operative in the later. Hence, spin orbital equations for the CCSD density [56] apply to the $\tilde{\rho}$ elements as well, provided the λ amplitudes are replaced by the ζ obtained by solving Eq. (15).

Most of the work of implementing EOM-CC energy gradients involves the reduced two-particle density matrix, ρ_{rs}^{pq}. Due to the presence of the non-linear exponential cluster operator as well as $\mathscr{L}$ and $\mathscr{R}$ in Eq. (25), a large number of terms contribute to each matrix element of ρ. Again, a diagrammatic approach seems to be best in identifying them, and antisymmetrized diagrams for both ρ_q^p and ρ_{rs}^{pq} are supplied in Figs. 2 and 3, respectively. For convenience, ρ_q^p and ρ_{rs}^{pq} are partitioned into all non-redundant subsets defined by the particle–hole character of p, q, r and s. Algebraic expressions for the reduced one- and two-particle density matrix, again following the Einstein summation convention and ordered to correspond precisely to the diagrammatic representations are

$$\rho_j^i = -l_e^i r_j^e - r_0 l_e^i t_j^e - \tfrac{1}{2} l_{ef}^{im} r_{jm}^{ef} - \tfrac{1}{2} r_0 l_{ef}^{im} t_{jm}^{ef} - l_{ef}^{im} r_m^f t_j^e + \delta_{ij}, \tag{30}$$

$$\rho_b^a = l_b^m r_m^a + r_0 l_b^m t_m^a + \tfrac{1}{2} l_{eb}^{mn} r_{mn}^{ea} + \tfrac{1}{2} r_0 l_{eb}^{mn} t_{mn}^{ea} + l_{eb}^{mn} r_m^e t_n^a, \tag{31}$$

$$\rho_a^i = r_0 l_a^i + l_{ae}^{im} r_m^e, \tag{32}$$

$$\begin{aligned}\rho_i^a = {} & t_i^a - l_e^m r_m^a t_i^e - l_e^m r_i^e t_m^a - \tfrac{1}{2} r_0 l_{ef}^{mn} t_{mn}^{ea} t_i^f - \tfrac{1}{2} r_0 l_{ef}^{mn} t_{mi}^{ef} t_n^a \\ & - \tfrac{1}{2} l_{ef}^{mn} r_i^f t_{mn}^{ea} - \tfrac{1}{2} l_{ef}^{mn} r_n^a t_{mi}^{ef} - \tfrac{1}{2} l_{ef}^{mn} r_{mn}^{ea} t_i^f - \tfrac{1}{2} l_{ef}^{mn} r_{mi}^{ef} t_n^a - l_{ef}^{mn} r_m^e t_i^f t_n^a \\ & + l_{ef}^{mn} r_m^e t_{in}^{af} - r_0 l_e^m t_i^e t_m^a + r_0 l_e^m t_{im}^{ae} + l_e^m r_{im}^{ae},\end{aligned} \tag{33}$$

$$\rho_{kl}^{ij} = \tfrac{1}{8} l_{ef}^{ij} r_{kl}^{ef} + \tfrac{1}{4} P_-(kl) l_{ef}^{ij} r_k^e t_l^f + \tfrac{1}{4} P_-(ij) P_-(kl) \delta_{ik} \delta_{jl}, \tag{34}$$

$$2\rho_{ka}^{ij} = -\tfrac{1}{2} l_{ea}^{ij} r_k^e, \tag{35}$$

$$\begin{aligned}2\rho_{jk}^{ia} = {} & -\tfrac{1}{2} l_e^i r_{jk}^{ea} - \tfrac{1}{2} P_-(jk) l_e^i r_j^e t_k^a - \tfrac{1}{2} P_-(jk) l_e^i r_k^a t_j^e + \tfrac{1}{2} P_-(jk) l_{fe}^{im} r_{jm}^{fa} t_k^e \\ & + \tfrac{1}{4} l_{fe}^{im} r_{jk}^{fe} t_m^a + \tfrac{1}{2} P_-(jk) l_{fe}^{im} r_k^e t_{jm}^{fa} + \tfrac{1}{4} l_{fe}^{im} r_m^a t_{jk}^{fe} - \tfrac{1}{2} P_-(jk) l_{fe}^{im} r_m^e t_j^f t_k^a\end{aligned}$$

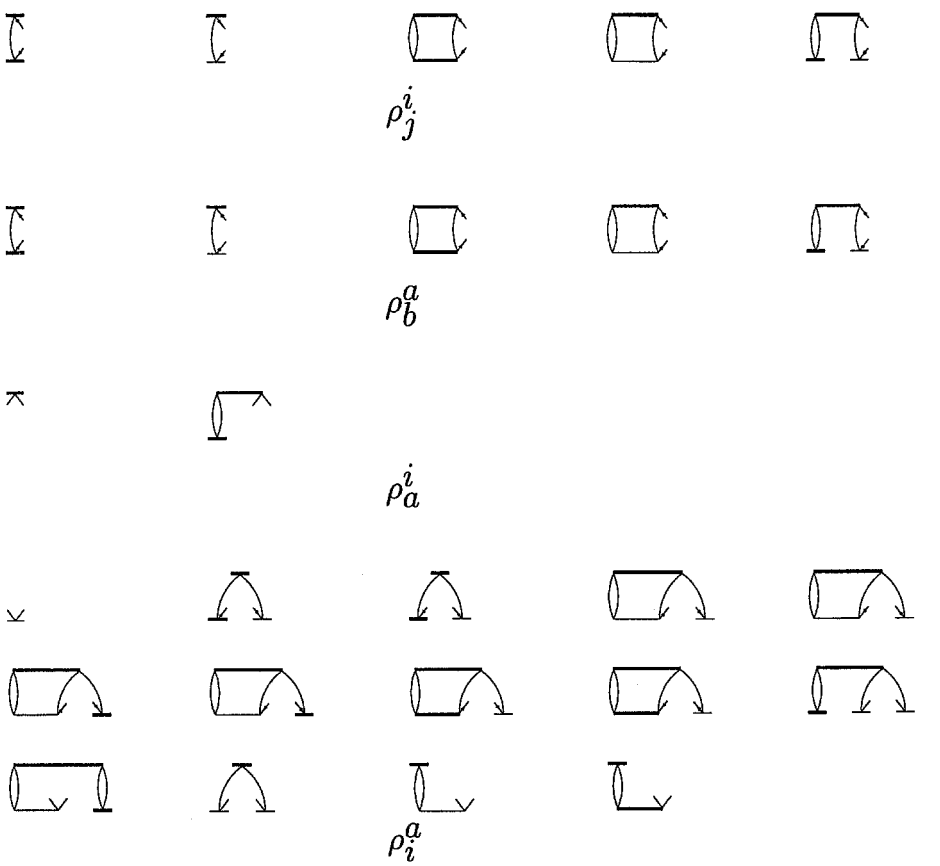

Fig. 2. Antisymmetrized diagrams for the EOM-CCSD reduced one-particle density matrix, ρ^p_q. The diagrammatic representation of $\mathscr{L}$, $\mathscr{R}$ and T operators is described in the caption to Fig. 1. Diagrams that contain $\mathscr{L}$ but neither $\mathscr{R}_1$ or $\mathscr{R}_2$ correspond to the r_0 contributions discussed in the text. The usual translation rules apply to these diagrams as well, but the values obtained by contracting the $\exp(T)$ with the $\mathscr{L}$ operator must be scaled by a factor of r_0. The t^a_i term in ρ^a_i is actually the sum of three contributions; this representation assumes that the bra and ket states have also been chosen to be biorthonormal $[\langle \mathscr{L} | \mathscr{R} \rangle = 1]$

$$
\begin{aligned}
&- \tfrac{1}{4} P_-(jk) l^{im}_{fe} r^a_k t^{fe}_{jm} - \tfrac{1}{4} P_-(jk) l^{im}_{fe} r^{fe}_{jm} t^a_k + \tfrac{1}{4} P_-(jk) l^{im}_{fe} r^a_m t^e_k t^f_j \\
&+ \tfrac{1}{2} P_-(jk) l^{im}_{fe} r^e_k t^a_m t^f_j - \tfrac{1}{2} l^{im}_{fe} r^e_m t^{fa}_{jk}, \qquad (36)
\end{aligned}
$$

$$
\begin{aligned}
4\rho^{ia}_{bj} = &- \tfrac{1}{4} P_-(ij) P_-(ab) l^i_b r^a_j - \tfrac{1}{4} P_-(ij) P_-(ab) l^{im}_{eb} r^{ea}_{jm} - \tfrac{1}{4} P_-(ij) P_-(ab) l^{im}_{eb} r^a_m t^e_j \\
&- \tfrac{1}{4} P_-(ij) P_-(ab) l^{im}_{eb} r^e_j t^a_m - P_-(ij) P_-(ab) l^{im}_{be} r^e_m t^a_j, \qquad (37)
\end{aligned}
$$

$$
\begin{aligned}
2\rho^{ab}_{ci} = &\tfrac{1}{2} l^m_c r^{ba}_{im} + \tfrac{1}{2} P_-(ab) l^m_c r^a_m t^b_i + \tfrac{1}{2} P_-(ab) l^m_c r^b_i t^a_m - \tfrac{1}{2} P_-(ab) l^{mn}_{ec} r^{ea}_{in} t^b_m \\
&- \tfrac{1}{4} l^{mn}_{ec} r^{ba}_{mn} t^e_i - \tfrac{1}{2} P_-(ab) l^{mn}_{ec} r^b_m t^{ea}_{in} - \tfrac{1}{4} l^{mn}_{ec} r^e_i t^{ba}_{mn} + \tfrac{1}{2} P_-(ab) l^{mn}_{ec} r^e_m t^b_i t^a_n \\
&+ \tfrac{1}{4} P_-(ab) l^{mn}_{ec} r^b_i t^{ea}_{mn} + \tfrac{1}{4} P_-(ab) l^{mn}_{ec} r^{ea}_{mn} t^b_i - \tfrac{1}{4} P_-(ab) l^{mn}_{ec} r^e_i t^b_m t^a_n \\
&- \tfrac{1}{2} P_-(ab) l^{mn}_{ec} r^b_m t^e_i t^a_n + \tfrac{1}{2} l^{mn}_{ec} r^e_m t^{ba}_{in}, \qquad (38)
\end{aligned}
$$

$$\rho_{kl}^{ij}$$

$$\rho_{ka}^{ij}$$

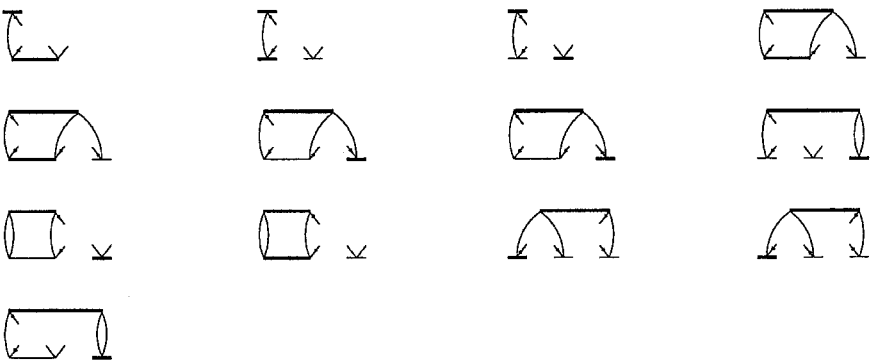

$$\rho_{jk}^{ia}$$

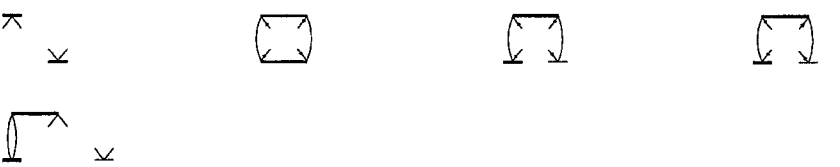

$$\rho_{bj}^{ia}$$

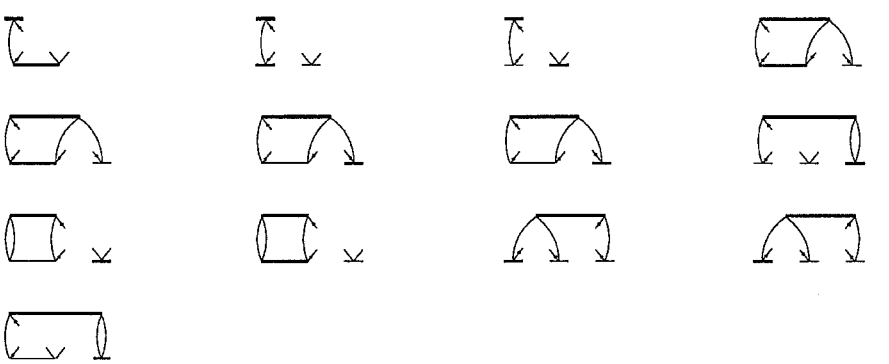

$$\rho_{ci}^{ab}$$

Fig. 3. Continued

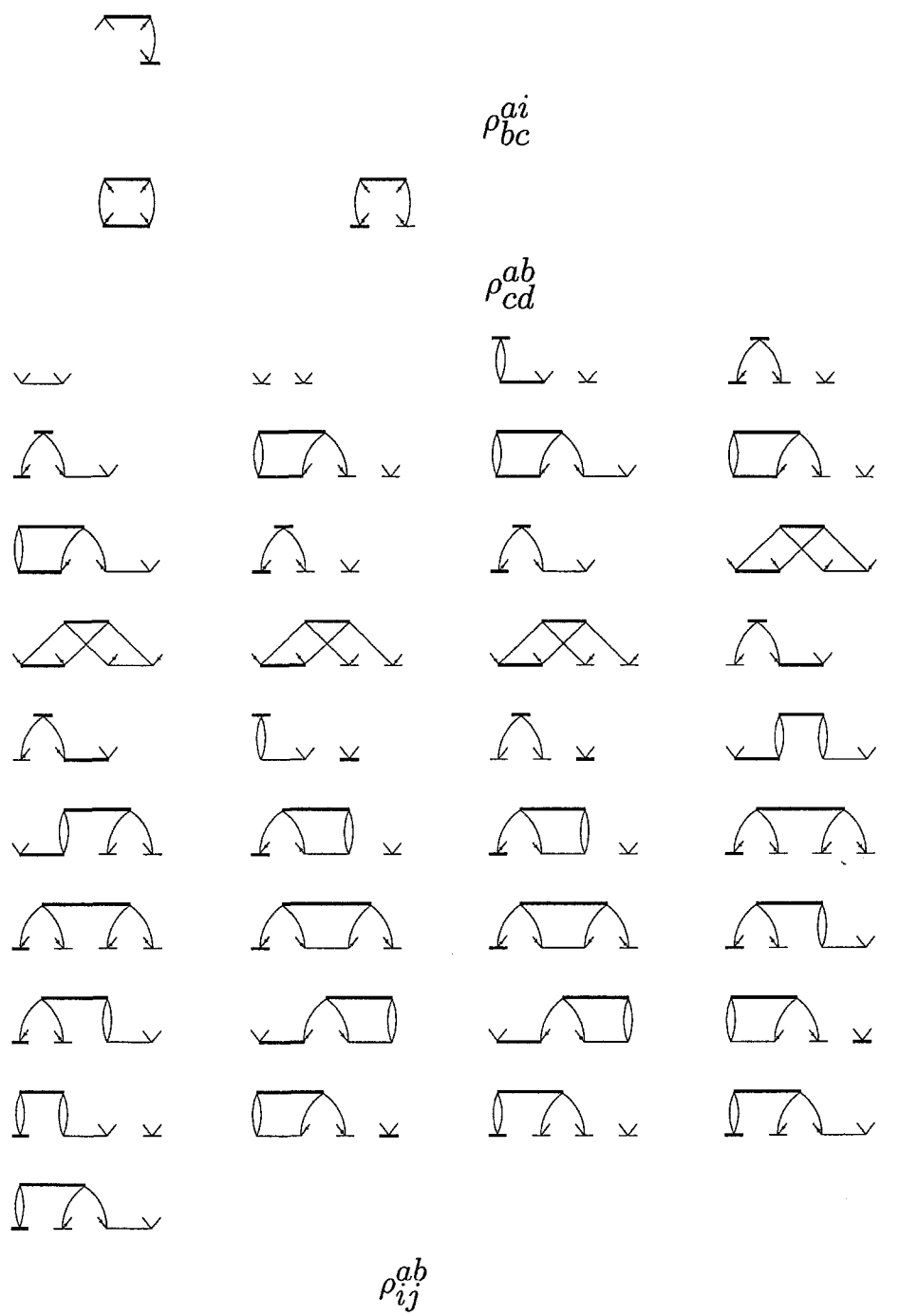

Fig. 3. Antisymmetrized diagrams for the EOM-CCSD reduced two-particle density matrix ρ_{rs}^{pq}. The diagrammatic representation of $\mathscr{L}$, $\mathscr{R}$ and T operators is described in the caption to Fig. 1. Excluded from this set of diagrams are the r_0 contributions discussed in the text

$$2\rho_{bc}^{ai} = \tfrac{1}{2} l_{bc}^{mi} r_m^a, \tag{39}$$

$$\rho_{cd}^{ab} = \tfrac{1}{8} l_{cd}^{mn} r_{mn}^{ab} + \tfrac{1}{4} P_-(ab) l_{cd}^{mn} r_m^a t_n^b, \tag{40}$$

$$\begin{aligned}
\rho_{ab}^{ij} = {} & \tfrac{1}{4} t_{ij}^{ab} + \tfrac{1}{8} P_-(ij) P_-(ab) t_i^a t_j^b + \tfrac{1}{4} P_-(ij) P_-(ab) l_e^m r_{im}^{ae} t_j^b \\
& - \tfrac{1}{4} P_-(ij) P_-(ab) l_e^m r_i^e t_m^a t_j^b - \tfrac{1}{4} P_-(ij) l_e^m r_i^e t_{mj}^{ab} - \tfrac{1}{8} P_-(ij) P_-(ab) l_{ef}^{mn} r_{mn}^{ea} t_i^f t_j^b \\
& - \tfrac{1}{8} P_-(ab) l_{ef}^{mn} r_{mn}^{ea} t_{ij}^{fb} - \tfrac{1}{8} P_-(ij) P_-(ab) l_{ef}^{mn} r_{im}^{fe} t_n^a t_j^b - \tfrac{1}{8} P_-(ij) l_{ef}^{mn} r_{im}^{fe} t_{nj}^{ab} \\
& - \tfrac{1}{4} P_-(ij) P_-(ab) l_e^m r_m^a t_i^e t_j^b - \tfrac{1}{4} P_-(ab) i_e^m r_m^a t_{ij}^{eb} \\
& + \tfrac{1}{16} l_{ef}^{mn} r_{ij}^{ef} t_{mn}^{ab} + \tfrac{1}{16} l_{ef}^{mn} r_{mn}^{ab} t_{ij}^{ef} + \tfrac{1}{16} P_-(ab) l_{ef}^{mn} r_{ij}^{ef} t_m^a t_n^b \\
& + \tfrac{1}{16} P_-(ij) l_{ef}^{mn} r_{mn}^{ab} t_i^e t_j^f - \tfrac{1}{4} P_-(ij) l_e^m r_{mj}^{ab} t_i^e - \tfrac{1}{4} P_-(ab) l_e^m r_{ij}^{eb} t_m^a \\
& + \tfrac{1}{4} P_-(ij) P_-(ab) l_e^m r_j^b t_{im}^{ae} - \tfrac{1}{4} P_-(ij) P_-(ab) l_e^m r_j^b t_i^e t_m^a \\
& + \tfrac{1}{4} P_-(ij) P_-(ab) l_{ef}^{mn} r_{im}^{ae} t_{jn}^{bf} - \tfrac{1}{4} P_-(ij) P_-(ab) l_{ef}^{mn} r_{im}^{ae} t_j^f t_n^b \\
& - \tfrac{1}{8} P_-(ij) P_-(ab) l_{ef}^{mn} r_i^f t_{mn}^{ea} t_j^b - \tfrac{1}{8} P_-(ij) P_-(ab) l_{ef}^{mn} r_n^a t_{mi}^{ef} t_j^b \\
& + \tfrac{1}{8} P_-(ij) P_-(ab) l_{ef}^{mn} r_i^e t_m^a t_n^b t_j^f + \tfrac{1}{8} P_-(ij) P_-(ab) l_{ef}^{mn} r_m^a t_i^e t_n^b t_j^f \\
& + \tfrac{1}{8} P_-(ij) l_{ef}^{mn} r_i^e t_{mn}^{ab} t_j^f + \tfrac{1}{8} P_-(ab) l_{ef}^{mn} r_m^a t_{ij}^{ef} t_n^b - \tfrac{1}{4} P_-(ij) P_-(ab) l_{ef}^{mn} r_n^a t_{jm}^{be} t_i^f \\
& - \tfrac{1}{4} P_-(ij) P_-(ab) l_{ef}^{mn} r_i^f t_{jm}^{be} t_n^a - \tfrac{1}{8} P_-(ij) l_{ef}^{mn} r_{in}^{ab} t_{jm}^{fe} - \tfrac{1}{8} P_-(ab) l_{ef}^{mn} r_{ij}^{af} t_{mn}^{eb} \\
& - \tfrac{1}{8} P_-(ij) P_-(ab) l_{ef}^{mn} r_j^b t_{mn}^{ea} t_i^f + \tfrac{1}{4} P_-(ij) P_-(ab) l_{ef}^{mn} r_m^e t_{in}^{af} t_j^b \\
& - \tfrac{1}{8} P_-(ij) P_-(ab) l_{ef}^{mn} r_j^b t_{im}^{fe} t_n^a - \tfrac{1}{4} P_-(ij) P_-(ab) l_{ef}^{mn} r_m^e t_i^f t_n^a t_j^b \\
& - \tfrac{1}{4} P_-(ij) l_{ef}^{mn} r_m^e t_{nj}^{ab} t_i^f - \tfrac{1}{4} P_-(ab) l_{ef}^{mn} r_m^e t_{ij}^{fb} t_n^a,
\end{aligned} \tag{41}$$

$$\rho_{ij}^{ab} = 0, \tag{42}$$

where terms involving the Kronecker delta (δ_{pq}) in Eqs. (30) and (34) represent the reference determinant contribution. The factors that appear on the left-hand side of the equations are a consequence of the unrestricted summation in Eq. (23) and are included to avoid overcounting.

Although complete algebraic expressions for the reduced one-particle density ρ_q^p are supplied above, diagrams and equations for the ρ_{rs}^{pq} are restricted to contributions from $\mathscr{R}$ operator elements that link the reference determinant $|0\rangle$ to bra states belonging to $\boldsymbol{g}$. In EOM-CC, $|0\rangle$ contributes [with weight r_0] to the wave function for excited states of the same symmetry due to the definition of $\mathscr{R}$ and the structure of $\bar{H}$. These "r_0 contributions" to the reduced two-particle density may be operationally grouped with the $\tilde{\rho}$ matrix elements since they are also defined by an equation that has the same form as the CCSD ground state density,

$$[\rho_{rs}^{pq}]_{r_0} = \langle 0 | \mathscr{L} \exp(-T) p^\dagger r q^\dagger s \exp(T) r_0 | 0 \rangle \tag{43}$$

$$= r_0 \langle 0 | \mathscr{L} \exp(-T) p^\dagger r q^\dagger s \exp(T) | 0 \rangle, \tag{44}$$

except that the l amplitudes replace the λ and all terms are scaled by a factor of r_0. The complete effective two-particle density matrix can therefore be conveniently

computed by evaluating the terms in Eqs. (34)–(41) and then adding the contribution

$$\langle 0 | \Delta \exp(-T) \exp(T) | 0 \rangle. \tag{45}$$

In Eq. (45), Δ is a composite operator

$$\Delta \equiv \mathscr{L} + r_0 \mathscr{L}, \tag{46}$$

whose definition is motivated by pragmatism rather than physical significance. The most demanding programming is associated with the first task, as an existing ground state CC gradient program can be used to evaluate Eq. (45) by simply using matrix elements of Δ instead of the λ amplitudes. This is precisely the strategy that has been adopted in our implementation.

3 Guidelines for implementation

Although relatively simple conceptually, gradient equations such as Eq. (23) are not appropriate for numerical computations due to the inconvenience of evaluating $\partial f_{pq}/\partial\chi$ and $\partial\langle pq \parallel rs\rangle/\partial\chi$ explicitly. These quantities depend upon the first-order response of both the electronic Hamiltonian [in the atomic orbital basis] and the molecular orbital coefficients. Ideally, one seeks a formulation that avoids the latter since differentiated one- and two-electron integrals are readily calculated in the atomic orbital basis by standard Gaussian integral programs. An elegant means for eliminating the orbital response contribution was introduced more than a decade ago by Handy and Schaefer [57]. In this "z-vector" method – which is closely related to the approach used to eliminate the T amplitude response in CCSD and EOM-CCSD gradient theories – a linear equation involving the orbital rotation gradient and the self-consistent field orbital Hessian is solved. The resulting solution can be considered as part of a one-particle effective density d_q^p. Combining this with the perturbation dependence of the atomic orbitals allows Eq. (23) to be rewritten as

$$\frac{\partial E}{\partial \chi} = \sum_{pq} d_q^p f_{qp}^{(\chi)} + \sum_{pqrs} D_{rs}^{pq} \langle rs \parallel pq \rangle^{\chi} + I_{pq} S_{pq}^{\chi} \tag{47}$$

where S_{pq}^{χ} and $\langle rs \parallel pq\rangle^{\chi}$ are derivatives of the atomic orbital overlap and antisymmetrized two-electron integrals transformed to the unperturbed molecular orbital representation, $f_{pq}^{(\chi)}$ are Fock matrix elements evaluated with differentiated integrals and the unperturbed reference determinant density matrix, and the I_{pq} coefficients serve to enforce orthonormality of the perturbed molecular orbitals. The z-vector and I_{pq} coefficients depend parametrically on both the unperturbed Hamiltonian and matrix elements of D. Apart from a dependence on D [and therefore ρ and $\tilde{\rho}$], solution of the z-vector equations in EOM-CCSD gradient calculations requires no new theoretical insight or programming.

The paragraph above underscores a point that was emphasized throughout the previous section, namely that an existing CCSD gradient program already contains much of the code needed to calculate EOM-CCSD energy derivatives provided the strategy outlined here is followed. Specifically, the only significant additional programming tasks are: (1) evaluation of the ξ_a^i and ξ_{ab}^{ij} amplitudes; (2) solution of

the $\mathscr{L}$ equation; and (3) computation of the reduced one- and two-particle density matrix. The remaining work consists of evaluating both $\tilde{\rho}$ and the "r_0 contributions" to ρ with the trick discussed at the end of Section 2 as well as straightforward interfacing to an existing CCSD gradient program. In our EOM-CCSD code (which has been incorporated in the ACES II program system [58]), the Ξ amplitudes and ρ are evaluated with vectorized matrix multiplication algorithms that fully exploit Abelian point group symmetry [59] while the ζ amplitudes are calculated by solving Eq. [15] with a standard algorithm for the iterative solution of linear equations [60]. Despite the relatively small number of discrete objectives that must be met to modify and extend an existing CCSD gradient program to calculate EOM-CCSD energy derivatives, a significant amount of effort is required due to the large number of terms that contribute to the Ξ and ρ matrix elements. Furthermore, effective treatment of symmetry requires some additional considerations since the contractions involve operators that do not necessarily transform according to the totally symmetric representation of the molecular point group [the overall symmetry of $\mathscr{L}$ and $\mathscr{R}$ is determined by the direct product of the ground and final state symmetries], while only totally symmetric quantities are encountered in CCSD gradient calculations.

While the equations presented in the previous section are in terms of the most fundamental wave function parameters [T, $\mathscr{L}$ and $\mathscr{R}$ amplitudes], considerable computational simplification is possible if suitable intermediates are precalculated and used in subsequent contractions. For example, in evaluating ρ_{ab}^{ij}, the fourth, fifth, eighth and ninth terms may be calculated at once by performing the contraction

$$\tfrac{1}{4} P_-(ij) \sum_m r_{mj}^{ab} \mathscr{G}_{mi}, \tag{48}$$

where

$$r_{mj}^{ab} \equiv t_{mj}^{ab} + P_-(ab) t_m^a t_j^b, \tag{49}$$

$$\mathscr{G}_{mi} \equiv -\sum_e l_e^m r_i^e - \tfrac{1}{2} \sum_{nef} l_{ef}^{mn} r_{ni}^{ef}. \tag{50}$$

It should be noted that the $\mathscr{G}$ intermediate is precisely equal to the first and third terms in the defining equation for the ρ_j^i elements (see Eq. (30)) and can also be used to simplify calculation of ρ matrix elements other than the ρ_{ab}^{ij} mentioned here. The choice of particular intermediates and the resulting computational scheme is a matter of choice, as no partitioning of terms will be optimal for all applications. For instance, a program intended for use on large molecules described by minimal or small split valence basis sets will benefit from a strategy that minimizes the number of contractions that involve a disproportionate number of occupied orbitals, but such an approach would not be wise for accurate large basis set calculations. However, some choice of intermediates should be used since a brute force diagram-by-diagram implementation is not efficient.

Selected properties of reduced density matrices and the exact treatment of certain systems that is possible with EOM-CCSD may be used to develop debugging strategies for the gradient code. Some techniques that were useful in checking the accuracy of our implementation are discussed below.

(i) As noted in the previous section, the Ξ amplitudes vanish when the EOM-CCSD method is exact. Thus, calculations for two classes of systems – those with fewer than three electrons and those described by basis sets so small that there are

only one or two virtual spin orbitals – can check on certain aspects of the computer code for Eqs. (19) and (20). In these cases, all contributions to the Ξ amplitudes represent exclusion principle violating terms and must therefore cancel exactly. While satisfaction of the condition $\xi_a^i = \xi_{ab}^{ij} = 0$ for these examples does not imply an absence of programming error, discrepancies can be helpful in identifying terms with incorrect factors and/or signs.

(ii) Although the EOM-CCSD reduced density matrix is not generally Hermitian due to the biorthogonal nature of the wave function representation, the proportionality of bra and ket states for cases in which the method is exact insures that the density matrix is symmetric. Hence, the examples used to check the Ξ amplitudes in (i) above can also test certain aspects of the code for the ρ_q^p and ρ_{rs}^{pq}. Again, it cannot be assumed that a symmetric density in the exact limit implies a correct implementation of the equations, but such a comparison does help to identify sign and factor errors.

(iii) The effective one-particle density matrix elements D_q^p can be rigorously tested by calculations of one-electron properties that suppress effects of orbital relaxation. For example, EOM-CCSD energies obtained in the presence of small positive and negative electric fields can be differentiated numerically to yield the dipole moment. Use of the zero-field molecular orbitals in the calculations excludes all orbital relaxation contributions and this "dipole moment" that should agree exactly with the dot product of D_q^p with the electric dipole integrals. As D_q^p depends upon both the reduced density and the ζ amplitudes, agreement between numerical and analytical calculation of this "unrelaxed" dipole moment suggests that both ρ_q^p and the Ξ matrix elements are correct.

(iv) A powerful check on the reduced one- and two-particle density matrices is to calculate the total electronic energy by contracting ρ with the bare Hamiltonian. If the energy obtained by this means agrees with the eigenvalue of $\bar{H}$ calculated by the EOM-CCSD energy code for several examples, the computer code for ρ is most probably correct. When disagreements are found, one useful approach for tracking down the error is provided by the following recipe. First, specific parts of the $\mathscr{L}$ or $\mathscr{R}$ vector are set to zero (for example, all r_i^a elements) and the quantity $\mathscr{L}\bar{H}\mathscr{R}$ is evaluated. This can then be compared to the "energy" calculated by evaluating the reduced density with this incorrect set of amplitudes and contracting it with the Hamiltonian. For example, if the energies agree only when the r_i^a amplitudes are assigned a value of zero, then at least one error is certainly present in parts of the code that involve the $\mathscr{R}_1$ amplitudes.

(v) In a spin orbital implementation of the equations, results for states based on closed shell reference determinants ($|0\rangle$) can be compared to those in which the calculation is run with an unrestricted Hartree–Fock (UHF) reference in which all orbitals are doubly occupied. This turns out to be particularly useful when the spin symmetry of restricted Hartree–Fock references is exploited throughout the program and contractions are carried out using spin-adapted amplitudes and $\bar{H}$ matrix elements. As no such spin adaptation is possible for true (open-shell) UHF calculations, separate code is required. Disagreement between results obtained with both choices of reference again facilitates the detection of programming errors.

(vi) A useful test for gradients based on open-shell UHF reference determinants is to compare results obtained with $N_\alpha > N_\beta$ (these refer to the number of α and β electrons, respectively) to those calculated when the spins are "reversed" $N_\beta > N_\alpha$.

(vii) The explicit treatment of symmetry in our implementation can also be used to advantage. For example, calculations for the water molecule can be performed in

full C_{2v} symmetry and the results can then be compared to those obtained from a run in which all symmetry is ignored. If the gradients do not agree exactly, then an error is present somewhere in the program. Results can then be compared subroutine by subroutine, which usually allows for a rapid identification of programming bugs.
(viii) Finally, the gradient can be compared to the result obtained by numerically differentiating energies obtained at displaced geometries. Using double-sided displacement techniques and strict convergence criteria for all iterative stages of the energy calculations (the ground state SCF and CCSD equations as well as the $\bar{H}$ eigenvalue solution), six to eight digits of precision can be obtained in numerically calculated derivatives. This provides a rather robust check on the gradient code, especially if comparisons are made for difficult cases in which correlation effects are very large (for example, the water molecule with r(O–H) $\approx$ 2 Å).

The discrete stages of the EOM-CCSD analytic energy derivative calculation are:

- Calculation of one- and two-electron integrals in the atomic orbital basis.
- Construction of the ground state zeroth-order Slater determinant $|0\rangle$, usually by solving the self-consistent field equations.
- Transformation of the atomic orbital integrals to the molecular orbital basis.
- Evaluation of the ground state CCSD wave function and calculation of the one- and two-body matrix elements of $\bar{H}$.
- Calculation of the right- and left-hand eigenvectors of $\bar{H}$ [$\mathscr{L}$ and $\mathscr{R}$] for the root under study.
- Computation of the ξ_a^i and ξ_{ab}^{ij} amplitudes.
- Solution of Eq. (15) for the ζ_a^i and ζ_{ab}^{ij} amplitudes.
- Evaluation of the reduced density matrix elements ρ.
- Calculation of $\tilde{\rho}$ and the "r_0 contributions" to ρ using the same program used for CCSD gradients.
- Transformation of the effective density matrix elements to the atomic orbital representation.
- Calculation of derivative overlap, one- and two-electron integrals in the atomic orbital representation. These are contracted "on the fly" with the effective density matrix elements and the I_{pq} to give the analytic derivative of the energy [44].

To conclude this section, a representative set of computational timings is presented in Table 1. In this example, an EOM-CCSD gradient calculation was performed for the first excited singlet state of vinylidene (C_2H_2) using a basis set of 78 contracted Gaussian functions on an IBM RS-6000/370 workstation. The reported CPU times clearly demonstrate that EOM-CCSD gradient calculations satisfy the most important criterion for applicability to physical problems, as the cost of evaluating the energy and its first derivatives with respect to nuclear displacements is less than twice that needed to calculate only the energy. Hence, this approach provides an efficient means for studying the potential energy surfaces of electronically excited states.

4 Application to formyl fluoride

Potential energy surfaces for low-lying excited states of formyl fluoride (HFCO) are of interest for several reasons. First, work by Weiner and Rosenfeld has shown that

photodissociation of this molecule occurs on the first excited singlet state (S_1) surface and involves loss of either the hydrogen of fluorine atom [61, 62]. This differs qualitatively from the thermal ground state dissociation of HFCO, in which HF and CO are produced in a single elementary step. In addition, the seminal work by Moore's group on mode specific (non-RRKM) unimolecular dissociation has used the S_1 state of HFCO as an intermediate in stimulated emission pumping experiments designed to probe highly excited vibrational levels of S_0 [63–66].

By analogy to the heavily studied formaldehyde molecule [67], the ground and (n, π^*) excited states of HFCO are expected to have significantly different equilibrium geometries. In the simplest molecular orbital description, excitation involves promotion of an electron to an anti-bonding π orbital that is concentrated on the carbon atom. This has two important qualitative implications for the excited state structure. First, the C–O bond length is expected to lengthen due to the reduction in formal bond order associated with occupation of the antibonding orbital. In addition, the planar (C_{2v} for CH_2O; C_s for HFCO) structure of the ground state species is not preserved in the excited states, as the carbon atom undergoes appreciable pyramidalization. Indeed, these qualitative expectations have been borne out in experimental studies of S_1 [69–71], as long vibrational progressions in the ν_2 carbonyl stretching and ν_6 "umbrella" mode are observed in the direct photoexcitation spectrum of HFCO. Furthermore, in stimulated emission pumping experiments [63–66], final states of S_0 reached after the system is permitted to evolve for a short time ($\approx$ 50 ns) on the S_1 surface are highly excited with respect to both ν_2 and ν_6. While this evidence for a non-planar S_1 structure is compelling, the best available set of geometrical parameters is based on a limited rotational analysis of the 2670 Å band system and was published a quarter century ago [70].

Despite a considerable body of theoretical work on the ground state surface of HFCO and its implications for the HFCO $\rightarrow$ HF + CO unimolecular process [72–75], the excited states have virtually been ignored. Indeed, no *ab initio* prediction of the potential energy surface and minimum energy structure of HFCO (S_1) has been published in the chemical literature. Accurate calculations for this system are needed, especially in view of the large uncertainties associated with the experimentally inferred structural parameters. It may be assumed that the lack of theoretical information regarding the S_1 state of HFCO results at least in part from the complexity of the potential energy surface. A tetratomic molecule with no non-trivial elements of symmetry has six internal degrees of freedom; exploration of the surface by means of energy calculations alone is not practical. Hence, the S_1 state of HFCO provides an illustrative example for demonstrating the power of the EOM-CCSD approach, as the availability of analytic energy derivatives for this method allows the properties and structure to be calculated in a straightforward and efficient manner. In this section, we present the first *ab initio* calculation of the equilibrium strucutre, harmonic vibrational frequencies and dipole moment components of HFCO in its first singlet excited (n, π^*) state.

In Table 2, optimized geometries, harmonic vibrational frequencies, infrared intensities, inertial axis dipole moment components and total energies are presented for both the $\tilde{X}^1A'$ (C_s) ground state and $\tilde{A}^1A(C_1)$ (n, π^*) excited state of HFCO. For the $\tilde{X}$ state, results are based on CCSD calculations carried out with a double-zeta plus polarization (DZP) basis set composed of Dunning's contractions [75] and a single set of polarization functions [p on hydrogen d on all other atoms] with exponents given in Refs. [76] and [77]. For the excited state, calculations were carried out at the EOM-CCSD level of theory with the same DZP basis set. Harmonic frequencies and infrared intensities (in the double harmonic

Table 2. Structural parameters and properties of the $\tilde{X}^1A'$ and $\tilde{A}^1A$ states of HFCO, obtained at the CCSD and EOM-CCSD levels, respectively, with the DZP basis set. τ is defined by the angle between the C–O bond and its projection onto the plane containing the carbon, hydrogen and fluorine atoms. Bond lengths are in Ångstroms, angles in degrees, harmonic frequencies in cm^{-1}, infrared intensities in km/mol, and dipole moment components in Debye

Parameter	$\tilde{X}^1A'$		$\tilde{A}^1A$	
	RHF-CCSD	Expt.	EOM-CCSD	Expt.
r_e (CO)	1.1874	1.095[a]	1.3462	1.36[d]
r_e (CF)	1.3403	1.338[a]	1.3458	1.34[d]
r_e (CH)	1.0997	1.181[a]	1.0977	1.10[d]
θ_e (OCF)	123.13	122.8[a]	109.82	110.[d]
θ_e (OCH)	127.35	127.3[a]	116.10	129.[d]
τ_e	180	180[a]	46.3	30–40[d]
ω_1 (CH stretch)	3173.51	2981.0[b]	3147.33	—
ω_2 (CO stretch)	1923.85	1836.9[b]	1217.57	1112[d]
ω_3 (HCO bend)	1418.33	1342.5[b]	1384.70	1286[d]
ω_4 (CF stretch)	1126.65	1064.8[b]	1149.10	—
ω_5 (FCO bend)	678.41	662.5[b]	462.35	450[d]
ω_6 (umbrella)	1046.72	1011.3[c]	996.45	924[d]
I_1	37.2	—	26.9	—
I_2	296.2	—	67.4	—
I_3	3.4	—	5.1	—
I_4	263.6	—	123.3	—
I_5	22.3	—	24.5	—
I_6	0.1	—	11.4	—
μ_a^e	—	—	0.476	—
μ_b^e	−2.042	—	−1.479	—
μ_c^e	0.621	—	0.020	—
Energy	−213.348514	—	−213.172010	—

[a] From Ref. [78]
[b] Fundamental frequencies from Ref. [79]
[c] Fundamental frequency from Ref. [65]
[d] Structure and fundamental frequencies from Ref. [70]
[e] Principal axis system coordinates are listed in Ref. [80]

approximation) were generated by numerical differentiation of analytic energy gradients and dipole moments obtained at geometries displaced from equilibrium along symmetry adapted internal coordinates.

The present calculations support the well-grounded belief that the S_1 state of HFCO adopts a non-planar geometry qualitatively similar to that seen in the analogous singlet excited state of formaldehyde [67]. The extent of pyramidalization (as measured by the angle τ defined in the caption to Table 2) inferred from the rotational analysis is somewhat less than that obtained in the EOM-CCSD calculations. Nevertheless, given that the structure of Ref. [70] is based on several assumptions necessitated by the incomplete nature of the data, agreement between EOM-CCSD and corresponding "experimental" geometrical parameters is satisfactory. A significant source of potential systematic error is the O–C–H bond angle,

which appears to close down by about 10° in the upper state. Since the constrained refinement of Fischer gives a value that is actually a few degrees larger than the ground state bond angle, further study of the experimental structure is warranted.

Calculated harmonic frequencies for the $\tilde{A}$ state are consistent with those inferred from vibrational progressions in the near-UV spectrum of Ref. [70]. In addition, the dominant internal coordinate description of normal modes are in accord with those assigned by Fisher [70], although calculations suggest that HCO bending and CO stretching are both involved in the upper state ν_2 and ν_3 modes. As one intuitively expects, the significant difference between ground and excited state structures is reflected in the normal mode frequencies. In particular, the carbonyl stretching frequency (ν_2) is much lower in the $\tilde{A}$ state, while the increased HCF bending frequency (ν_5) may be attributed to the large reduction in the excited state bond angle (116° vs. 127° in the ground state).

Once the excited state geometry and harmonic force field are known, adiabatic excitation energies may be calculated. When corrected for vibrational zero-point energies, the resulting electronic term values (T_0) can be compared with 0–0 band origins that are either observed directly or extrapolated from vibrational progressions. This provides a good check on the accuracy of the excited state treatment and is somewhat more satisfying than comparing theoretical vertical excitation energies to the position of absorption maxima, especially in cases where large and qualitatively significant geometry changes take place. While calculation of T_0 values for diatomics and highly symmetrical small molecules is not particularly demanding, it must be emphasized that the structure and vibrational frequencies can be calculated economically for the S_1 state of HFCO only when analytic gradient methods are used. With the DZP basis set, the theoretical EOM-CCSD term value for the $\tilde{A}^1A \leftarrow \tilde{X}^1A'$ excitation process is $T_0 = 4.74$ eV, in excellent agreement with the experimentally measured threshold energy of 4.65 eV (37488 cm^{-1}). The accurate prediction of T_0 at the EOM-CCSD level with a DZP basis set and the good agreement between calculated and observed vibrational frequencies indicate that the S_1 state of formyl fluoride is quite satisfactorily treated by this economical level of approximation.

The exploratory study of the HFCO (S_1) potential energy surface reported here augments a growing body of work in which EOM-CCSD gradient methods have been used to successfully study electronically excited states and their properties. Already, this new theoretical tool has been used to investigate the first excited state of acetylene [29], to predict threshold energies and vibrational progressions in the photodetachment spectrum of the vinylidene anion [30], and to identify pathways for HCN → HNC isomerization in the two lowest excited states of that system [34]. Given the wide scope of unsolved questions in photochemistry and electronic spectroscopy, it is logical to conclude that applications of EOM-CCSD will be reported with increasing frequency in the next few years. For problems that require some consideration of excited state structures or potential energy surfaces, the efficient gradient formulation documented here represents an invaluable extension to the basic method.

Acknowledgements. This work was partially supported by a grant from the Robert A. Welch Foundation (F-1283) [J.F.S]; a Young Investigator Award from the National Science Foundation [J.F.S]; and a "Liebig-Stipendium" from the Fonds der Chemischen Industrie [J.G.]. J.G. also wishes to thank R. Ahlrichs for generous support.

References

1. See, for example, review articles by Werner H-J (p. 1); Shepard R (p. 62); Ross BO (p. 399) 1987 In: Lawley KP (ed.) Ab initio methods in quantum chemistry, Part II, Wiley, New York
2. Kim K, Shavitt I, Del Bene JE (1992) J Chem Phys 96:7573; Del Bene J, Kim K, Shavitt I (1991) Can J Chem 69:246, and references therein
3. Szalay PG, Karpfen A, Lischka H (1990) Chem Phys 141:355, and references therein
4. Pacchioni G, Koutecky J (1988) J Chem Phys 1066: and references therein
5. Bruna PJ, Peyerimhoff SD (1987) Adv Chem Phys 67:1 (1987), and references therein
6. Davidson ER, McMurchie LE (1979) in: Excited States Vol. 5, Academic, New York, p 1, and references therein
7. Serrano-Andres L, Merchan M, Nebot-Gil I, Lindh R, Roos BO (1993) J Chem Phys 98:3151, and references therein
8. Serrano-Andres L, Merchan M, Nebot-Gil I, Roos BO, Fülscher M (1993) J Am Chem Soc 115:6184, and references therein
9. See, for example, McLean AD, Lengsfeld BH, Pacansky J, Ellinger Y (1985) J Chem Phys 83:3567, Englebrecht L, Liu B (1983) J Chem Phys 78:3907
10. Monkhorst HJ (1977) Int J Quantum Chem (Symp) 11:421
11. Mukherjee D, Mukherjee PK (1979) Chem Phys 39:325
12. Emrich K (1981) Nucl Phys A 351:379
13. Ghosh S, Mukherjee D (1984) Proc Ind Acad Sci 93:947
14. Sekino H, Bartlett RJ (1984) Int J Quantum Chem (Symp.) 18:255
15. Takahashi M, Paldus J (1986) J Chem Phys 85:1486
16. Geertsen J, Rittby M, Bartlett RJ (1989) Chem Phys Lett 164:57
17. Koch H, Jørgensen P (1990) J Chem Phys 93:3333
18. Koch H, Jensen HJAa, Helgaker T, Jørgensen P (1990) J Chem Phys 93:3345
19. Stanton JF, Bartlett RJ (1993) J Chem Phys 98:7029
20. Comeau DC, Bartlett RJ (1993) Chem Phys Lett 207:414
21. Rico RJ, Lee TJ, Head-Gordon M (1994) Chem Phys Lett 218:139
22. The SAC-CI method of Nakatsuji and coworkers may also be viewed as an approximate EOM-CCSD procedure. See Nakatsuji H (1978) Chem Phys Lett 39:562
23. Although the CC state used to parameterize the similarity transformed Hamiltonian is referred to the "ground state" throughout this paper, it need not correspond to the actual electronic ground state. While the term "reference state" might be preferable in some respects, it also leads to potential confusion between the CC state and its zeroth-order Slater determinant approximation.
24. Rigorously speaking, the ground and final states form a non-interacting biorthogonal set.
25. Purvis GD, Bartlett RJ (1982) J Chem Phys 76:1910
26. The question of size-consistency and size-extensivity considerations in the EOM-CC and closely related linear response CC approaches (see Refs. [17] and [18]) has been a popular subject of discussion in the literature [see, for example, Meissner L, Bartlett RJ (1991) J Chem Phys 94:6670]; while these methods formally involve unlinked diagrams in the energy expression, energies are size-consistent (in the sense that energy levels of isolated molecules persist in a supermolecule environment) as clearly demonstrated by Koch et al. in Ref. [18]. Somewhat relevant to the present work is a recent investigation of size consistency criteria for the reduced and effective n-particle density matrices of EOM-CC theory [Stanton JF J Chem Phys, in press] 101:8928 (1994)
27. An improved description of both ground and excited states in asymptotic regions of the potential energy surface can be achieved by including triple excitation effects, albeit with a significant corresponding increase in computational cost. The first extension of EOM-CC to include effects of the T_3 cluster operator has been reported recently [Watts JD, Bartlett RJ J Chem Phys, in press].
28. Stanton JF, Bartlett RJ (1993) J Chem Phys 98:9335
29. Stanton JF, Huang CM, Szalay PG (1994) J Chem Phys 101:356 (1994)
30. Stanton JF, Gauss J J Chem Phys 101:3001 (1994).
31. Oliphant N, Bartlett RJ (1994) J Amer Chem Soc 116:4091
32. See, for example, Fogarasi G, Pulay P (1983) In: Vibrational spectral and vibrational structure, Vol. 14, Durig J (ed.), Reidel, Dordrecht

33. Stanton JF (1983) J Chem Phys 99:8840
34. Stanton JF, Gauss J (1994) J Chem Phys 100:4695
35. Cizek J (1966) J Chem Phys 45:4256
36. J. Cizek (1966) Adv Chem Phys 14:35
37. Scuseria GE, Scheiner AC, Lee TJ, Rice JE, Schaefer HF (1987) J Chem Phys 86:2881
38. Adamowicz L, Laidig WD, Bartlett RJ (1984) Int J Quantum Chem (Symp) 18:245
39. Bartlett RJ (1986) In: Geometrical derivatives of energy surfaces and molecular properties, Jørgensen P, Simons J (eds) Reidel, Dordrecht
40. Scheiner AC, Scuseria GE, Rice JE, Lee TJ, Schaefer HF (1987) J Chem Phys 87:5361
41. Scuseria GE, Schaefer HF (1988) Chem Phys Lett 146:23
42. Salter EA, Trucks GW, Bartlett RJ (1989) J Chem Phys 90:1752
43. Koch H, Jensen HJAa, Helgaker T, Jørgensen P, Scuseria GE, Schaefer HF (1990) J Chem Phys 92:4924
44. Gauss J, Stanton JF, Bartlett RJ (1991) J Chem Phys 95:2623
45. Gauss J, Lauderdale WJ, Stanton JF, Watts JD, Bartlett RJ (1991) Chem Phys Lett 182:207
46. Gauss J, Stanton JF, Bartlett RJ (1991) J Chem Phys 95:2639
47. Scuseria GE (1991) J Chem Phys 94:442
48. Lee TJ, Rendell AP (1991) J Chem Phys 94:6229
49. Watts JD, Gauss J, Bartlett RJ (1992) Chem Phys Lett 200:1; (1993) J Chem Phys 98:8718
50. Arponen JS (1983) Ann Phys (NY) 151:311
51. Dalgarno A, Stewart AL (1958) Proc Roy Soc A247:245
52. Kucharski SA, Bartlett RJ (1986) Adv Quntum Chem 18:281
53. The one- and two-particle character of the bare Hamiltonian is not preserved under the similarity transformation that relates H and $\bar{H}$. For CCSD, the latter contains up to six-body terms, but only one-, two- and three-body terms are encountered in the EOM-CCSD description of excited states. Techniques for avoiding the explicit construction and storage of the three-body terms are discussed in Ref. [19], but these quantities do not contribute to the Ξ amplitudes.
54. For a readable and pedagogical discussion of this point, see Nooijen M, Ph.D. Thesis, Vrije Universiteit, Amsterdam, 1992; and Nooijen M, Snyders JC (1993) Int J Quantum Chem 47:3
55. See, for example, Blaizot JP, Ripka G (1986) Quantum theory of finite systems, MIT Press, Cambridge pp 610–618
56. Algebraic equations for two-particle density elements in terms of fundamental wave function parameters are documented for the CCSDT method in Table II of Ref. [42], where they are designated by $\Gamma(pq;rs)$ instead of the D_{rs}^{pq} notation used here. The terms that define the CCSD density are those that involve only the Λ_1, Λ_2, T_1 and T_2 amplitudes. Unlike the formulation of the present work, the equations of Ref. [42] do not reflect the characteristic asymmetry of the CC density since the D_{jk}^{ia}, D_{bc}^{ai} and D_{ab}^{ij} elements have been grouped with D_{ka}^{ij}, D_{ci}^{ab} and D_{ij}^{ab}, respectively. It should be emphasized that evaluation of gradients and molecular properties involves contraction of D with a Hermitian operator, and there is therefore no numerical effect associated with symmetrization of the density. Indeed, it is computationally advantageous to do so, since separate storage of quantities such as D_{bc}^{ai} and D_{ci}^{ab} can significantly increase disk storage requirements. Algebraic equations for the CCSD one-particle density matrix are given in Ref. [46].
57. Handy NC, Schaefer HF (1984) J Chem Phys 51:5031
58. ACES II, an *ab initio* program system, authored by Stanton JF, Gauss J, Lauderdale WJ, Watts JD, Bartlett RJ. The package also contains modified versions of the MOLECULE Gaussian integral program of Almlöf J, Taylor PR, the ABACUS integral derivative program written by Helgaker TU, Jensen HJAa, Jørgensen P, Taylor PR and the PROPS property integral code of Taylor PR
59. Stanton JF, Gauss J, Watts JD, Bartlett RJ (1991) J Chem Phys 94:4334
60. Pople JA, Krishnan R, Schlegel HB, Binkley JS (1979) Int J Quantum Chem (Symp.) 13:255
61. Weiner BR, Rosenfeld RN (1988) AIP Conf Proc 191:648
62. Weiner BR, Rosenfeld RN (1988) J Chem Phys 92:4640
63. Choi YS, Moore CB (1989) J Chem Phys 90:3875
64. Choi YS, Teal P, Moore CB (1990) J Opt Soc Amer 7:1829
65. Choi YS, Moore CB (1991) J Chem Phys 94:5414
66. Choi YS, Moore CB (1992) J Chem Phys 97:1010
67. See, for example, Moule DC, Walsh AD (1975) Chem Rev 75:67

68. Giddings LE, Innes KK (1961) J Mol Spectr 6:528
69. Giddings LE, Innes KK (1962) J Mol Spectr 8:328
70. Fischer G J Mol Spectr (1969) 29:37
71. Green WH, Jayatilaka D, Willets A, Amos RD, Handy NC (1990) J Chem Phys 93:4965
72. Kamiya K, Morokuma K (1992) J Chem Phys 94:7287
73. Francisco JS, Zhao Y (1992) J Chem Phys 96:7587
74. Wei T-G, Wyatt RE (1993) J Phys Chem 97:13580
75. Dunning TH (1971) J Chem Phys 55:716
76. Redmon LT, Purvis GD, Bartlett RJ (1979) J Amer Chem Soc 101:2856 [exponents for C, H and O]
77. Stanton JF, Lipscomb WN, Magers DH, Bartlett RJ (1989) J Chem Phys 90:3241 [exponent for F]
78. Huisman PA, Klebe KJ, Mijlhoff FC, Renes GH (1979) J Mol Struct 57:71
79. Herzberg G (1966) Electronic spectra of polyatomic molecules, Van Nostrand Reinhold, New York
80. Principal axis coordinates (a, b, c) for the two electronic states are (in atomic units): O: (0, 0.4069, − 2.1836); C: (0, − 0.7753, − 0.2765); F: (0, 0.2980, 2.0171); H: (0, − 2.8438, − 0.7569) [$\tilde{X}^1A'$]; O: (0.0369, 0.4744, − 2.2027); C: (− 0.1782, − 1.0156, − 0.1520); F: (0.0303, 0.3877, 1.9588); H: (0.9668, − 2.7453, − 0.1569) [$\tilde{A}^1A$]